



저작자표시-비영리-변경금지 2.0 대한민국

이용자는 아래의 조건을 따르는 경우에 한하여 자유롭게

- 이 저작물을 복제, 배포, 전송, 전시, 공연 및 방송할 수 있습니다.

다음과 같은 조건을 따라야 합니다:



저작자표시. 귀하는 원저작자를 표시하여야 합니다.



비영리. 귀하는 이 저작물을 영리 목적으로 이용할 수 없습니다.



변경금지. 귀하는 이 저작물을 개작, 변형 또는 가공할 수 없습니다.

- 귀하는, 이 저작물의 재이용이나 배포의 경우, 이 저작물에 적용된 이용허락조건을 명확하게 나타내어야 합니다.
- 저작권자로부터 별도의 허가를 받으면 이러한 조건들은 적용되지 않습니다.

저작권법에 따른 이용자의 권리는 위의 내용에 의하여 영향을 받지 않습니다.

이것은 [이용허락규약\(Legal Code\)](#)을 이해하기 쉽게 요약한 것입니다.

[Disclaimer](#)

의학박사 학위 논문

자궁 경부암 마우스 모델에서 렌바티닙과
항 PD-1의 항종양 효과에 대한 연구

Anti-tumor effects of lenvatinib plus anti-PD-1 in
syngeneic murine cervical cancer models

울산대학교 대학원

의학과

강지식

자궁 경부암 마우스 모델에서 렌바티닙과
항 PD-1의 항종양 효과에 대한 연구

지도교수 김 용 만

이 논문을 의학박사 학위 논문으로 제출함

2023 년 8 월

울 산 대 학 교 대 학 원

의 학 과

강 지 식

강지식의 의학박사학위 논문을 인준함

심사위원 이 신 화 인

심사위원 김 용 만 인

심사위원 김 대 연 인

심사위원 김 주 현 인

심사위원 김 문 흥 인

울 산 대 학 교 대 학 원

2023 년 8 월

Abstract

Anti-tumor effects of lenvatinib plus anti-PD-1 in syngeneic murine cervical cancer models.

Jisik Kang

Department of Obstetrics and Gynecology,

Graduated School, University of Ulsan

Background

Immune checkpoint inhibitors (ICIs) have been used in patients with various solid tumors since they were approved by the U.S. FDA in 2011, but only less than 20% of them benefit from ICIs, including anti-programmed cell death protein 1 (anti-PD-1). Recently, many attempts to improve the response of ICIs are in progress. In particular, the vascular endothelial growth factor receptor (VEGFR) pathway has emerged as a major target, which has synergistic anti-tumor effects with ICIs by regulating the differentiation of tumor-associated macrophages, antigen-presenting dendritic cells, and T cell infiltration in VEGFRi. In this study, the effects of lenvatinib combined with anti-PD-1 were evaluated in a syngeneic murine model of uterine cervical cancer to demonstrate whether VEGFR inhibition enhances the anti-tumor effects of ICIs.

Materials and methods

To evaluate the synergistic effects of lenvatinib and anti-PD-1, a syngeneic mouse model of cervical cancer was used. A total of 1×10^7 U14 cells were injected subcutaneously into the flanks of BALB/c wild-type and nude mice. They were treated with lenvatinib (10 mg/kg, orally, daily) until the tumor volume reached 200 mm^3 , and then anti-PD-1 (200 μg per mouse, intraperitoneally (I.P.), twice a

week) was administered to immunocompetent mice for 3 weeks. Tumor volume was measured twice a week. At the end of the experiment, tumors and spleens were harvested and histological analysis was performed.

Results

Tumor volume was significantly reduced by lenvatinib in the immunocompetent model (278 mm³ in Len vs. 490 mm³ in Veh) ($p = 0.0156$); in particular, the tumor size decreased after 2 weeks of injection. In study, the synergistic effects of lenvatinib and anti-PD-1 were also confirmed in immune mouse models. Each single treatment group showed a reduction in tumor volume compared to the vehicle group (Len: 278 mm³; anti-PD-1: 258 mm³; Veh: 490 mm³). Furthermore, the lenvatinib plus anti-PD-1 group showed reduced tumor volume to 110 mm³ on the 24th day after injection, which was significantly different compared to each single treatment group ($p = 0.0078$ and $p = 0.0078$, respectively).

Conclusions

In this study, the anti-tumor effects of anti-PD-1 were enhanced by the modulation of the tumor microenvironment with lenvatinib in immunocompetent murine cervical cancer models. In conclusion, the addition of lenvatinib is expected to increase the efficacy of ICIs in patients with cervical cancer who are resistant or insensitive to ICIs.

Keywords: cervical cancer; lenvatinib; anti-PD-1; immune checkpoint inhibitors.

Contents

Abstract	i
Contents	iii
List of Figures	iv
Introduction	1
Materials and Methods	3
Results	6
Discussion	14
Conclusion	15
References	16
Korean abstract	19

List of Figures

Figure 1. Inhibition of U14 cell line growth and migration by lenvatinib treatment.	9
Figure 2. Lenvatinib anti-tumor activity in the immunocompetent U14 model	10
Figure 3. Regulation of immune cells by lenvatinib in an immunocompetent U14 model	11
Figure 4. Synergistic anti-tumor activity of lenvatinib and anti-PD-1 in U14 immuno-competent model	12
Figure 5. Regulation of immune cells in TME by synergistic anti-tumor activity of lenvatinib and anti-PD-1 in U14 immuno-competent model	13

Introduction

Immune checkpoint inhibitors (ICIs) have been approved by the U.S. FDA since 2011 for the treatment of various solid tumors ⁽¹⁾, but less than 20% of patients benefit from them, including anti-programmed cell death protein 1 (anti-PD-1) ^(2, 3).

Programmed cell death protein-1 (PD-1) is a receptor found on the surface of immune cells that plays a crucial role in regulating immune responses. PD-1, when bound to its ligands PD-L1 or PD-L2, inhibits T cell activity and prevents excessive immunity activation ⁽⁴⁾. Cancer cells can engage PD-1 on T cells, inhibiting their activity and allowing tumors to escape destruction ⁽⁵⁾. The anti-PD-1 therapy aims to overcome this immune evasion strategy employed by cancer cells. By blocking the interaction between PD-1 and its ligands, anti-PD-1 antibodies unleash the immune system's ability to effectively recognize and attack cancer cells ⁽⁶⁾. However, as described above, it is effective only in approximately 20-30% of cancers, and thus many studies are being conducted to increase the therapeutic effect.

The vascular endothelial growth factor receptor (VEGFR) pathway has emerged as one of the main targets for enhancing cooperative anticancer effects ^(7, 8). The VEGFR pathway exerts cooperative anticancer effects with ICI by regulating the differentiation of tumor-associated macrophages, antigen-presenting dendritic cells and infiltrating T cells in VEGFRi ^(9, 10).

Lenvatinib is a multiple receptor tyrosine kinase inhibitor that mainly targets vascular endothelial growth factor (VEGF) and fibroblast growth factor (FGF) receptors, platelet-derived growth factor receptor alpha (PDGFRA)⁽¹¹⁾. Anti-PD-1 antibodies, on the other hand, target the programmed cell death-1 (PD-1) receptor on T-cells, preventing tumor cells from evading the immune system ⁽³⁾. The combination of lenvatinib and anti-PD-1 antibodies has been shown to modulate

cancer immunity in the tumor microenvironment (TME) by reducing tumor-associated macrophages (TAMs) and enhancing anti-tumor activity via the interferon (IFN) signaling pathway ⁽¹²⁾. Lenvatinib reduces angiogenesis and may overturn the immunosuppressive effects of VEGF in the TME, whereas anti-PD-1 antibodies prevent tumor cells from evading the immune system ⁽¹³⁾. The combination of lenvatinib and anti-PD-1 antibodies works to target multiple pathways in the TME and enhance anti-tumor activity via modulation of cancer immunity and angiogenesis ⁽¹⁴⁾.

Studies have reported promising results for the combination therapy of lenvatinib and anti-PD-1 antibodies in various cancer types, including hepatocellular carcinoma and thyroid cancer^{(15) (16)}. Study was investigated the effectiveness of lenvatinib combined with anti-PD-1 in syngeneic murine cervical cancer model to show whether VEGFRi improves ICI anti-tumor effect.

Materials and methods

Cell line

The murine uterine cervical cancer cell line (MUCC) was obtained from MedPacto (Seoul, Republic of Korea). The cells were maintained at 37°C with 5% CO₂ in Dulbecco's modified Eagle's medium (DMEM) (Gibco) containing 10% fetal bovine serum and 1% penicillin/streptomycin.

Cell viability assay

U14 cells were seeded in 96-well plates at a density of 5×10^2 cells per well. Plates were incubated for one day in an incubator to allow cells to adhere to the surface. Cells were treated with different concentrations of lenvatinib (0.625, 1.25, 2.5, 5, and 10 mM). Plates were incubated at 37 °C for 24 h – 72 h. Cell viability was assessed after drug treatment for 24, 48, or 72 h using Cell titer glo 2.0 (Promega, Madison MI, USA). Luminescence was measured with a microplate reader.

Cell migration assay

Cells were cultured at 1×10^6 cells/well in 6-well plates and then incubated for one day. A wound was made using a 200 µL pipette tip. Cell debris was removed by washing with PBS and then treated with lenvatinib (0, 1.25 mM). Wound intervals were captured microscopically at constant times (0, 24, and 48 h).

Model establishment & drug treatment

BALB/c mice (6-7 weeks old) were purchased from JA BIO (Suwon, Republic of

Korea). All mice were bred in a specific pathogen-free (SPF) animal facility at the Asan Institute for Life Science (Seoul, Republic of Korea). We established syngeneic mouse models of cervical cancer to confirm the synergistic effects of lenvatinib combined with anti-PD-1. A total of 1×10^7 U14 cells were injected subcutaneously into the flanks of BALB/c wild-type (immunocompetent) and nude (immunocompromised) mice. The animals were treated with lenvatinib until the tumor volume reached 200 mm^3 , and subsequently, anti-PD-1 was administered to immunocompetent mice. Lenvatinib (10 mg/kg, orally, daily) and anti-PD-1 (200 μg per mouse, intraperitoneally (I.P.), twice a week) were administered for 3 weeks. Tumor volume was measured twice a week. Tumor size was measured as follows: tumor volume (mm^3) = length (mm) \times width (mm) \times width (mm)/2. At the end of the experiment, tumors and spleens were harvested and histological analysis was performed.

Immunofluorescence

Slides were prepared using formalin-fixed paraffin-embedded (FFPE) tissues. The slides were placed in a stainless-steel staining rack and dried overnight in a dry oven at 60°C for deparaffinization, twice in 100% xylene for 10 min, twice in 100% ethanol for 5 min, once in 90% ethanol for 5 min, 80% ethanol for 5 min, 70% ethanol for 5 min, 60% ethanol for 5 min, 50% ethanol for 5 min, and then washed three times with PBS. The antigen was exposed to sodium citrate buffer (0.3% Tris-sodium citrate, 0.5% Tween 20 in D.W. at pH 6.0) and processed with blocking solution (5% bovine serum albumin in PBS) for 1 h. The samples were incubated at 4°C overnight with the following antibodies: APC anti-mouse I-A/I-E antibody (clone M5/114.15.2, BioLegend), FITC anti-mouse F4/80 antibody (clone BM8, BioLegend), FITC anti-mouse CD11c antibody (clone N418, BioLegend), PE anti-mouse CD86 antibody (clone GL-1, BioLegend), FITC anti-mouse CD4 antibody (clone RM4-4, BioLegend), and PE anti-mouse FOXP3 antibody (clone MF-14,

BioLegend). Cell nuclei were counterstained with DAPI dilactate (D9564-10MG, Sigma-Aldrich).

Statistical analysis

Differences between the combination group, vehicle group, and each single treatment group were analyzed using the Wilcoxon signed-rank test. An unpaired t-test with Welch's correction was used for the migration assay. All P-values were two-sided, and a value <0.05 was considered statistically significant. Statistical analyses were performed using Prism (v5.03, Graph Pad Software, San Diego, California, USA).

Results

Lenvatinib exhibits anti-tumor activity by reducing the survival and migration of cervical cancer cell lines.

Lenvatinib is an anti-angiogenic drug and anticancer agent ⁽¹⁷⁾. In tumor cells, lenvatinib induces apoptosis by reducing survival and migration ⁽¹⁸⁾. Study was performed cell viability and migration assays using the U14 cervical cancer cell line. Study was determined whether lenvatinib could reduce the survival and migration of tumor cells in vitro. Murine uterine cervical cancer cell lines were cultured in DMEM and are shown in micrographs ($\times 4$ and $\times 10$) (**Figure 1A**). The viability of U14 cells treated with lenvatinib in vitro was measured at different time points (24–72 h). Compared to vehicle, the viability was 1.04%, 11.12%, and 17.04% at 0.625 μM , 0.84%, 11.28%, and 23.66% at 1.25 μM , 0%, 14.26%, and 25.97% at 2.5 μM , 4.83% at 5 μM , 11.28% and 23.66%, decreasing to 4.83%, 11.28%, and 23.66% at 10 μM (24 h, 48 h, and 72 h, respectively) (**Figure 1B**). In the cell migration assays, observed 24 h and 48 h after lenvatinib treatment, the migration ability of the lenvatinib group (205%) was significantly lower than that of the vehicle group (236%) ($p < 0.05$, $p < 0.0001$) (**Figure 1C**)

Lenvatinib shows remarkable anti-tumor activity in an immunocompetent model.

To evaluate the anti-tumor activity of lenvatinib, immune activity was modulated by using immunocompetent mice (BALB/c wild-type mice) and immunocompromised mice (BALB/c nude mice) as U14 cervical cancer models. In the immunocompromised model, tumor growth was inhibited by 20% in the lenvatinib group compared to the vehicle group on day 17 of injection (2914 mm^3 vs. 3663 mm^3 , respectively) ($p = 0.0938$) (**Figure 2A**). In contrast, in the

immunocompetent model, lenvatinib significantly reduced tumor volume by 43% (278 mm³ in Len vs. 490 mm³ in Veh) ($p = 0.0156$), and tumor size decreased 2 weeks after injection (**Figure 2B**). In particular, the immunocompetent model showed enhanced anti-tumor activity compared to the immunocompromised model. (**Figure 2A and 2B**). In BALB/c wild-type mice, lenvatinib significantly reduced the tumor size compared to the vehicle (**Figure 2C**).

Lenvatinib activates the immune system by recruiting TAMs and maturing dendritic cells in the TME.

To investigate whether lenvatinib modulates the immune system in an immunocompetent setting, it was extracted lenvatinib from the tumors of BALB/c wild-type mice and histologically analyzed the immune cells present in the TME. Lenvatinib treatment significantly increased the fluorescence intensity of M1-like TAMs (F4/80+, I-A/I-E+) compared to that in the vehicle group (880.3%) ($p = 0.0021$) (**Figure 3A**). In addition, lenvatinib significantly increased (1088.7%) the average fluorescence intensity of mature dendritic cells (CD11c+, CD86+) in the tumor, confirming that mDC recruitment was improved compared to that in the vehicle group ($p = 0.0063$) (**Figure 3B**). These results show that lenvatinib activates tumor-suppressor immune cells in cervical cancer.

In an immunocompetent model, lenvatinib and anti-PD-1 show synergistic anti-tumor effects.

Based on the immune system-activating effects of lenvatinib, study was investigated the synergistic anti-tumor effects of the combination of lenvatinib and anti-PD-1 in an immunocompetent model⁽¹⁹⁾. Each single treatment group showed a reduction in tumor volume compared to the vehicle group ($p = 0.0234$ and $p =$

0.0078,). In addition, the lenvatinib and anti-PD-1 combination treatment group reduced the tumor volume to 110 mm³ on the 24th day after injection, showing a significant difference compared to each single treatment group ($p = 0.0078$ and $p = 0.0078$, respectively) (**Figure 4A**). Tumor size also decreased in the single treatment group of lenvatinib and anti-PD-1, but more significantly in the combination treatment group (**Figure 4B**). This indicates that lenvatinib potentially increases anti-PD-1 sensitivity in a mouse cervical cancer cell line model.

The synergistic anti-tumor effects of lenvatinib and anti-PD-1 activate immune cells in the TME.

As mentioned above, based on the assumption that treatment with lenvatinib potentially enhances anti-PD-1 sensitivity in the MUCC model, treatment with lenvatinib and anti-PD-1 was similarly effective in the TME in single treatment and combination treatment groups. To determine whether U14 tumors regulate immune cells, immunofluorescence assays were performed. First, the average fluorescence intensity increased by 880.3% and 539% in M1-like TAMs (F4/80+, I-A/I-E+) compared to vehicle in single treatment with lenvatinib and anti-PD-1, respectively ($p = 0.0021$ and $p=0.0246$). The combination treatment group increased significantly by 224.2% and 366.4% compared to each single treatment group ($p = 0.0348$ and $p = 0.0220$) (**Figure 5A**). In addition to showing M1-like TAMs, the combination treatment group also showed significantly increased mDCs (CD11c+, CD86+) within the TME relative to the monotherapy and vehicle groups ($p = 0.0348$, $p = 0.0220$, and $p = 0.0002$) (**Figure 5B**). In contrast, T regulatory cells (CD4+, Foxp3+) decreased by 51%, 57.2%, and 93.5% in the single treatment group, lenvatinib and anti-PD-1, and the combined treatment group, respectively, compared to the vehicle ($p = 0.0006$, $p = 0.0066$, $p = 0.0066$, $p < 0.0001$), and the combination treatment group significantly decreased by 86.8% and 85 %, respectively, compared to each single treatment group ($p=0.0012$, $p=0.0164$) (**Figure 5C**).

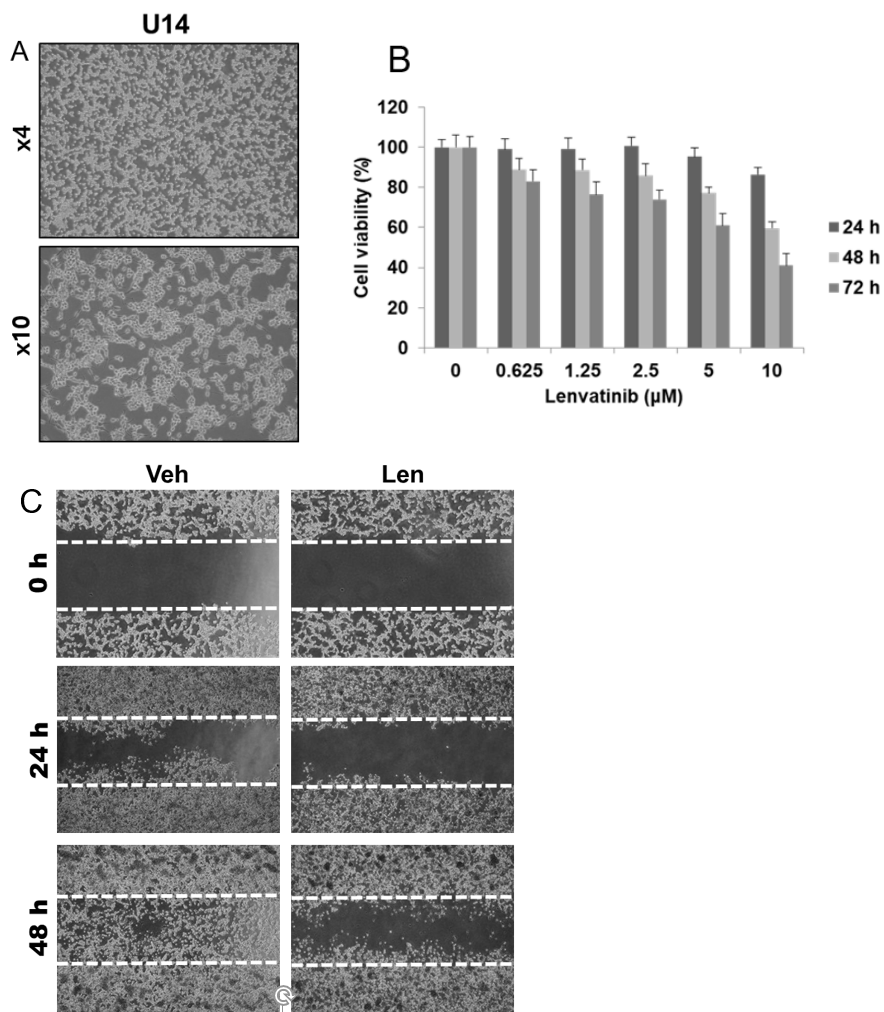


Figure 1. Inhibition of U14 cell line growth and migration by lenvatinib treatment.

A) U 14 cell line image (magnification: $\times 4$, $\times 10$).

B) Cell viability was analyzed by CellTiter-Glo. Treatment of U14 cells with lenvatinib (0, 0.625, 1.25, 2.5, 5, and 10 μM) showed dose-dependent and time-dependent inhibitory effects for 24 h, 48 h, and 72 ho. Error bars are shown as mean \pm SEM.

C) Microscopic images of changes in the wound area (white dotted line) at 0 h, 24 h, and 48 h after vehicle and lenvatinib (1.25 μM) treatment (top)(magnification: $\times 4$). The average number of cells in the wound area over time of the vehicle and lenvatinib groups is shown as a bar graph (bottom)(n = 3). Error bars are shown as mean \pm SEM. Statistical analysis was performed using a two-way ANOVA test with Graph Pad Prism 5. $p < 0.05$, * $p < 0.01$, *** $p < 0.001$ compared with 24 h.

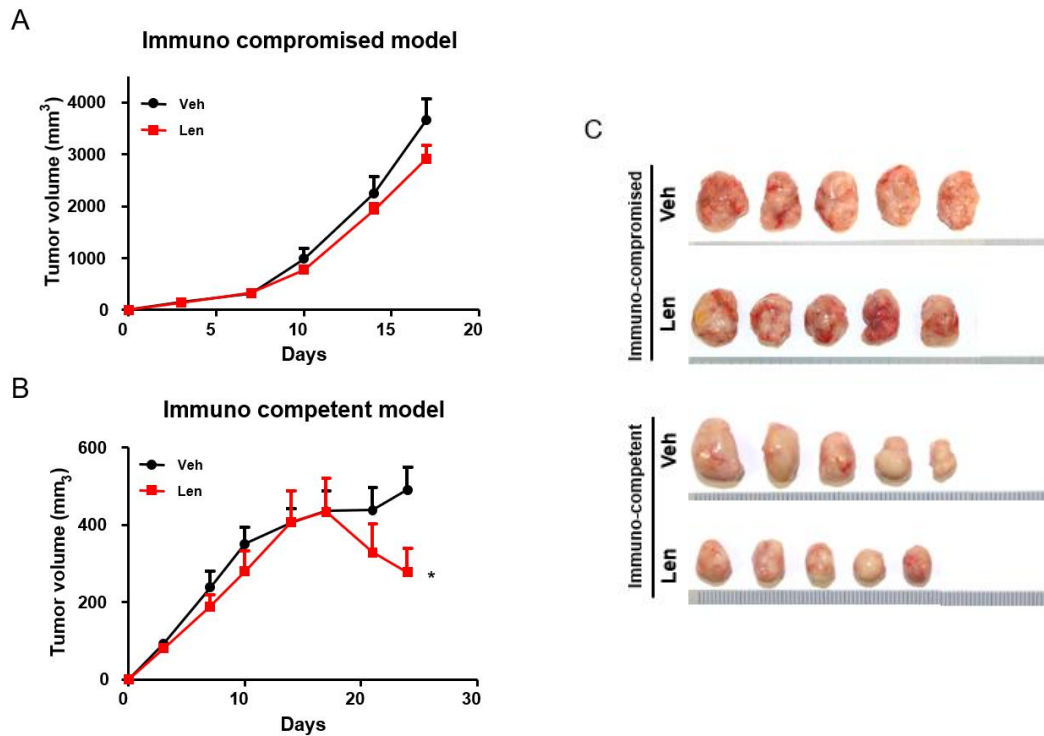


Figure 2. Lenvatinib anti-tumor activity in the U14 immunocompetent model. A, B). The U 14 cell line was subcutaneously injected into immunocompetent (BALB/c wild-type) and immunocompromised (BALB/c nude) mice, and on day 7, they were divided into vehicle and lenvatinib groups (Day 7 mean tumor volume: BALB/c nude mice, 327.4 mm³; BALB/c wild-type mice, 212.8 mm³). Lenvatinib was administered orally daily at 10 mg/kg. Vehicle (black circles) (n = 10) and lenvatinib (red squares) (n = 10), represent the mean tumor volume. Tumor volume was measured on days 3, 7, 10, 14, and 17 in BALB/c nude mice and on days 3, 7, 10, 14, 17, 21, and 24 in BALB/c wild-type mice. Error bars are shown as mean \pm SEM. Statistical analysis was performed using Wilcoxon signed-rank test with Graph Pad Prism 5. *p<0.05 compared with vehicle. C). Representative tumor pictures of the vehicle and lenvatinib groups are shown in U 14 immunocompetent mice (BALB/c wild-type mice) model (top) and immunocompromised mice (BALB/c nude mice) model (bottom).

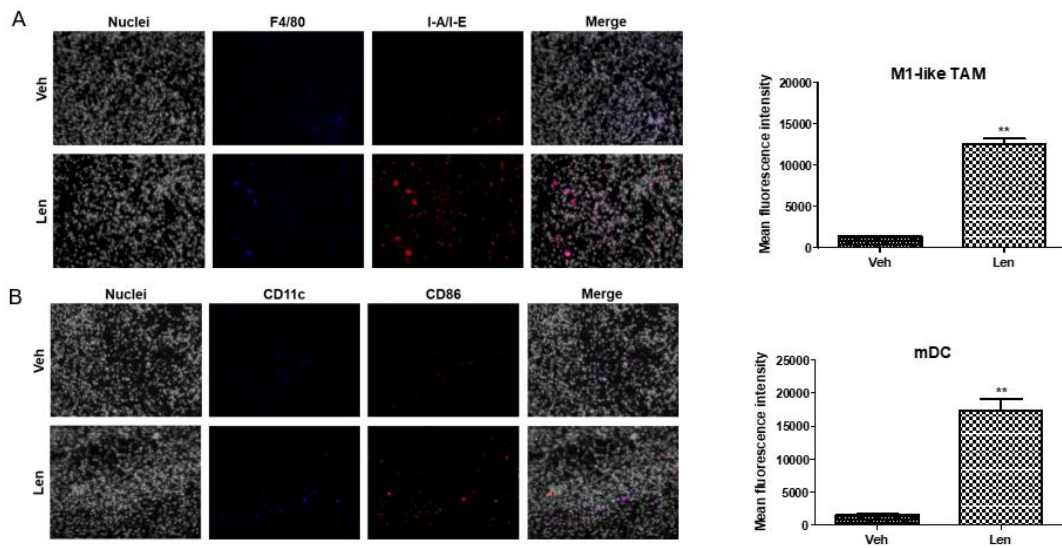


Figure 3. Regulation of immune cells by lenvatinib in the U14 immunocompetent model.

A, B). On the 24th day of the U14 immunocompetent mice (BALB/c wild-type mice), tumor tissue was harvested. Expression of F4/80+ I-A/I-E+ M1-like tumor-associated macrophages (M1-like TAMs), CD11c+ and CD86+ mature dendritic cells (mDCs) in tumor tissue is shown using immunofluorescence analysis (right) (magnification: $\times 20$). Mean fluorescence intensity per area of M1-like TAMs and mDCs in the vehicle and lenvatinib groups was photographed in three sections under a microscope and is presented as a bar graph (left) ($n = 3$). Error bars are shown as mean \pm SEM. Statistical analysis was performed using unpaired t-tests with Welch's correction with Graph Pad Prism 5. ** $p < 0.01$ compared with vehicle.

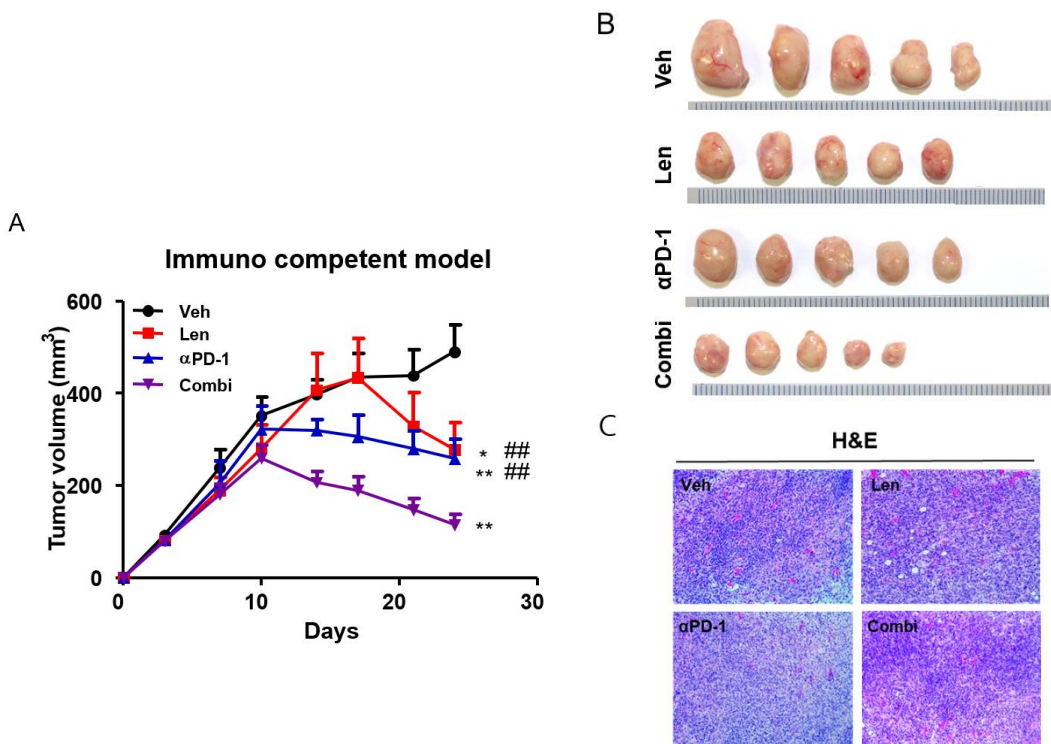


Figure 4. Synergistic anti-tumor activity of lenvatinib and anti-PD-1 in the U14 immunocompetent model.

A). The U 14 cell line was subcutaneously injected into immunocompetent mice (BALB/c wild-type mice), and on day 7, they were divided into four groups (vehicle, lenvatinib, anti-PD-1, combination of lenvatinib plus anti-PD-1) (Day 7 mean tumor volume: 201.6 mm³). Lenvatinib was administered orally at 10 mg/kg daily, and anti-PD-1 was administered intraperitoneally at 200 µg twice a week. Vehicle (black circles) (n = 9), lenvatinib (red squares) (n = 10), anti-PD-1 (blue triangles)(n = 9), combination of lenvatinib plus anti-PD-1 (purple inverted triangles)(n = 10) represent the mean tumor volume. Tumor volume was measured on days 3, 7, 10, 14, 17, 21, and 24. Error bars are shown as mean ± SEM. Statistical analysis was performed using Wilcoxon signed-rank test with Welch's correction with Graph Pad Prism 5. * p<0.05, ** p<0.01 compared with vehicle; ## p<0.01 compared with combination therapy.

B). Representative tumor images of the vehicle, lenvatinib, ant-PD-1, and combination groups are shown.

C). Representative images of each group stained with H&E by tumor tissue section (magnification: ×20).

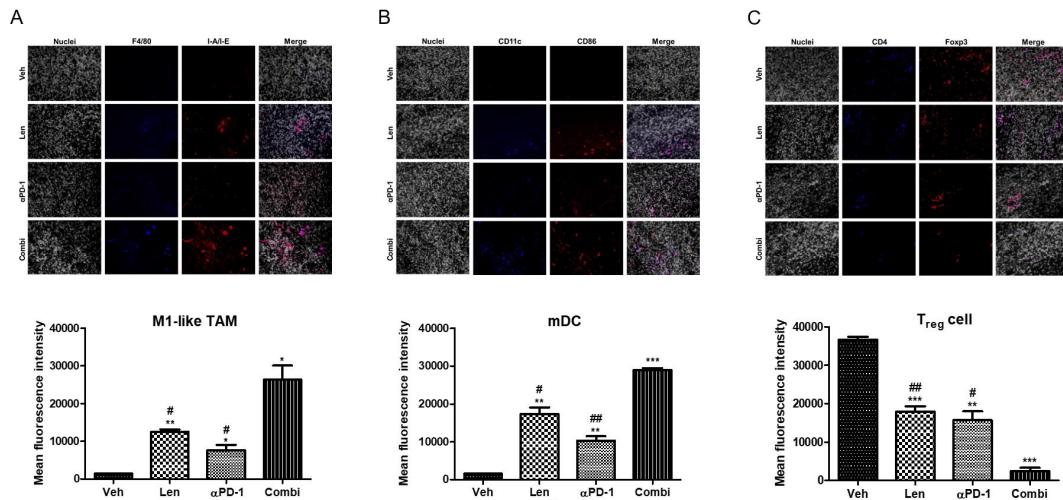


Figure 5. Regulation of immune cells in the TME by the synergistic anti-tumor activity of lenvatinib and anti-PD-1 in the U14 immunocompetent model.

A, B, and C). Tumor tissue was harvested from U14 immunocompetent mice (BALB/c wild-type mice). Expression of F4/80+ I-A/I-E+ tumor-associated macrophages (TAMs), CD11c+ CD86+ mature dendritic cells (mDCs), and CD4+ Foxp3+ T regulatory cells in tumor tissue is shown using immunofluorescence analysis (top) (magnification: $\times 20$). Mean fluorescence intensity per area of M1-like TAM and mDC in four group studies (vehicle, lenvatinib, anti-PD-1, and combination of lenvatinib plus anti-PD-1) were photographed in three sections under a microscope and are presented as a bar graph (bottom) ($n=3$). Error bars are shown as mean \pm SEM. Statistical analysis was performed using unpaired t-tests with Welch's correction with Graph Pad Prism 5. $p < 0.05$, * $p < 0.01$, *** $p < 0.001$ compared with vehicle; # $p < 0.05$, ## $p < 0.01$ compared with combination therapy.

Discussion

In this study, the synergistic effect of combining lenvatinib with anti-PD-1 was confirmed. The study aimed to investigate the efficacy of the combination therapy in treating cervical cancer by assessing the syngeneic effect. Combination therapy also demonstrated anti-tumor effects through the activation of immune cells in the TME. The results demonstrated synergistic effects when anti-PD-1 was used in combination with lenvatinib in a mouse model of cervical cancer.

VEGF stimulated by hypoxia in the TME induces tumor angiogenesis, resulting in malformed and dysfunctional vascular structures⁽²⁰⁾. During this process, dendritic cell (DC) maturation is inhibited, compromising antigen presentation effectiveness and disrupting T cell priming^{(21) (22)}. Additionally, TAMs polarize from an immunosuppressive M1-like phenotype to an immunosuppressive M2-like phenotype^{(23) (24)}. Regulatory T (Treg) cells also accumulate within the TME and promote tumor angiogenesis⁽²⁵⁾. In our study, through immunofluorescence assays, study was confirmed that the distribution of M1-like TAMs and mature DCs in the U14 cell line increased in lenvatinib monotherapy and lenvatinib and anti-PD-1 combination therapy compared to vehicle. In addition, the Treg distribution decreased. Thus, lenvatinib activates the immune system by recruiting TAMs and mDCs in the TME.

Previous studies have investigated the mechanisms and effects of lenvatinib and anti-PD-1 combination therapy. Kato et al. showed that lenvatinib, a VEGFR and FGFR signaling inhibitor, reduced the number of TAMs and showed stronger anti-tumor activity when combined with PD-1 blockade, affecting the anti-tumor immune response in melanoma and colorectal cancer cells^{(12) (26)}. Torrens et al. showed that lenvatinib and anti-PD-1 exerted unique immunomodulatory effects in hepatocellular cancer cells by activating immune pathways, reducing Treg cell infiltration, and suppressing TGF β signaling⁽²⁷⁾.). In another clinical trial, KEYNOTE-

775 patients with advanced endometrial cancer treated with pembrolizumab and lenvatinib had a longer progression-free survival than those treated with chemotherapy. Combination therapy was also associated with a higher objective response rate than chemotherapy ⁽²⁸⁾.

This study has some limitations. The pathways of receptors other than VEGF that respond to lenvatinib in the TME were not studied, and neither the levels of cytokines and chemokines nor the presence of other immune cells that respond to this process were investigated. In addition, further research is needed to evaluate combination therapy treatment effects according to the expression levels of PD-L1. Although many microenvironment cells were not identified, M1 TAMs, DCs, and Tregs, which perform a significant role in combination therapy, were identified, and meaningful results were obtained.

Conclusion

Our study found that lenvatinib exhibited anti-tumor activity in an MUCC cell line by reducing cancer cell survival through the recruitment of M1 TAMs and mDCs. In addition, the anti-tumor effect was further increased when used as a combination therapy with anti-PD-1 in an immunocompetent mouse model. Combination therapy has demonstrated increased synergistic effects and improved outcomes in animal models and clinical trials. Further studies on the detailed mechanism and clinical studies targeting actual patients with cervical cancer are needed.

References

1. Vaddepally RK, Kharel P, Pandey R, Garje R, Chandra AB. Review of indications of FDA-approved immune checkpoint inhibitors per NCCN guidelines with the level of evidence. *Cancers*. 2020;12(3):738.
2. Hamid O, Robert C, Daud A, Hodi FS, Hwu W-J, Kefford R, et al. Safety and tumor responses with lambrolizumab (anti-PD-1) in melanoma. *New England Journal of Medicine*. 2013;369(2):134-44.
3. McDermott DF, Atkins MB. PD-1 as a potential target in cancer therapy. *Cancer medicine*. 2013;2(5):662-73.
4. Liu J, Chen Z, Li Y, Zhao W, Wu J, Zhang Z. PD-1/PD-L1 Checkpoint Inhibitors in Tumor Immunotherapy. *Front Pharmacol*. 2021;12:731798.
5. Seidel JA, Otsuka A, Kabashima K. Anti-PD-1 and Anti-CTLA-4 Therapies in Cancer: Mechanisms of Action, Efficacy, and Limitations. *Front Oncol*. 2018;8:86.
6. Wang Z, Wu X. Study and analysis of antitumor resistance mechanism of PD1/PD-L1 immune checkpoint blocker. *Cancer Med*. 2020;9(21):8086-121.
7. Chen HX, Cleck JN. Adverse effects of anticancer agents that target the VEGF pathway. *Nature reviews Clinical oncology*. 2009;6(8):465-77.
8. Goel HL, Mercurio AM. VEGF targets the tumour cell. *Nat Rev Cancer*. 2013;13(12):871-82.
9. Afroj T, Mitsuhashi A, Ogino H, Saijo A, Otsuka K, Yoneda H, et al. Blockade of PD-1/PD-L1 pathway enhances the antigen-presenting capacity of fibrocytes. *The Journal of Immunology*. 2021;206(6):1204-14.
10. Wculek SK, Cueto FJ, Mujal AM, Melero I, Krummel MF, Sancho D. Dendritic cells in cancer immunology and immunotherapy. *Nature Reviews Immunology*. 2020;20(1):7-24.
11. Roskoski Jr R. The role of small molecule platelet-derived growth factor receptor (PDGFR) inhibitors in the treatment of neoplastic disorders. *Pharmacological research*. 2018;129:65-83.
12. Kato Y, Tabata K, Kimura T, Yachie-Kinoshita A, Ozawa Y, Yamada K, et al. Lenvatinib plus anti-PD-1 antibody combination treatment activates CD8+ T cells through reduction of tumor-associated macrophage and activation of the interferon pathway. *PLoS One*. 2019;14(2):e0212513.
13. Le TMD, Yoon A-R, Thambi T, Yun C-O. Polymeric Systems for Cancer Immunotherapy: A Review. *Frontiers in Immunology*. 2022;13:826876.
14. Gunda V, Gigliotti B, Ashry T, Ndishabandi D, McCarthy M, Zhou Z, et al. Anti-PD-1/PD-L1 therapy augments lenvatinib's efficacy by favorably altering the immune microenvironment of murine anaplastic thyroid cancer. *International Journal of Cancer*.

2019;144(9):2266-78.

15. Wu JY, Wu JY, Li YN, Qiu FN, Zhou SQ, Yin ZY, et al. Lenvatinib combined with anti-PD-1 antibodies plus transcatheter arterial chemoembolization for neoadjuvant treatment of resectable hepatocellular carcinoma with high risk of recurrence: A multicenter retrospective study. *Front Oncol.* 2022;12:985380.
16. Bertol BC, Bales ES, Calhoun JD, Mayberry A, Ledezma ML, Sams SB, et al. Lenvatinib Plus Anti-PD-1 Combination Therapy for Advanced Cancers: Defining Mechanisms of Resistance in an Inducible Transgenic Model of Thyroid Cancer. *Thyroid.* 2022;32(2):153-63.
17. Capozzi M, De Divitiis C, Ottaiano A, von Arx C, Scala S, Tatangelo F, et al. Lenvatinib, a molecule with versatile application: from preclinical evidence to future development in anti-cancer treatment. *Cancer Management and Research.* 2019;11:3847.
18. Zhang D, Zhang Y, Cai Z, Tu Y, Hu Z. Dexamethasone and lenvatinib inhibit migration and invasion of non-small cell lung cancer by regulating EKR/AKT and VEGF signal pathways. *Experimental and therapeutic medicine.* 2020;19(1):762-70.
19. Crespo-Rodriguez E, Bergerhoff K, Bozhanova G, Foo S, Patin EC, Whittock H, et al. Combining BRAF inhibition with oncolytic herpes simplex virus enhances the immune-mediated antitumor therapy of BRAF-mutant thyroid cancer. *Journal for ImmunoTherapy of Cancer.* 2020;8(2).
20. Lee WS, Yang H, Chon HJ, Kim C. Combination of anti-angiogenic therapy and immune checkpoint blockade normalizes vascular-immune crosstalk to potentiate cancer immunity. *Experimental & molecular medicine.* 2020;52(9):1475-85.
21. Yao Y, Li P, Singh P, Thiele AT, Wilkes DS, Renukaradhya GJ, et al. Vaccinia virus infection induces dendritic cell maturation but inhibits antigen presentation by MHC class II. *Cellular immunology.* 2007;246(2):92-102.
22. Jhunjhunwala S, Hammer C, Delamarre L. Antigen presentation in cancer: insights into tumour immunogenicity and immune evasion. *Nature Reviews Cancer.* 2021;21(5):298-312.
23. Huang Y, Yuan J, Righi E, Kamoun WS, Ancukiewicz M, Nezivar J, et al. Vascular normalizing doses of antiangiogenic treatment reprogram the immunosuppressive tumor microenvironment and enhance immunotherapy. *Proceedings of the National Academy of Sciences.* 2012;109(43):17561-6.
24. Peng L, Wang Y, Fei S, Wei C, Tong F, Wu G, et al. The effect of combining Endostar with radiotherapy on blood vessels, tumor-associated macrophages, and T cells in brain metastases of Lewis lung cancer. *Translational Lung Cancer Research.* 2020;9(3):745.
25. Ohue Y, Nishikawa H. Regulatory T (Treg) cells in cancer: Can Treg cells be a new therapeutic target? *Cancer science.* 2019;110(7):2080-9.

26. Frey B, Rückert M, Weber J, Mayr X, Derer A, Lotter M, et al. Hypofractionated irradiation has immune stimulatory potential and induces a timely restricted infiltration of immune cells in colon cancer tumors. *Frontiers in immunology*. 2017;8:231.
27. Torrens L, Montironi C, Puigvehí M, Mesropian A, Leslie J, Haber PK, et al. Immunomodulatory effects of lenvatinib plus anti-programmed cell death protein 1 in mice and rationale for patient enrichment in hepatocellular carcinoma. *Hepatology*. 2021;74(5):2652-69.
28. Makker V, Colombo N, Casado Herráez A, Santin AD, Colomba E, Miller DS, et al. Lenvatinib plus pembrolizumab for advanced endometrial cancer. *New England Journal of Medicine*. 2022;386(5):437-48.

국문요약

연구배경 및 목적

면역관문억제제는 2011년 미국 FDA의 승인을 받은 이후 다양한 고형암 환자에게 적용되어 왔지만 항프로그래밍화 세포사 단백질-1(항 PD-1)을 포함한 면역관문억제제의 효과를 보는 환자는 20-30%에 불과하다. 최근 면역관문억제제의 반응성을 개선하기 위한 많은 연구가 진행되고 있으며, 특히 혈관내피증식인자 수용체(VEGFR)의 경로는 종양 관련 대식세포의 분화를 조절하고 항원 제시 수지상 세포 및 혈관내피증식인자 수용체 억제제(VEGFRi)에서 T 세포의 침윤을 통한 면역관문억제제와 상승적인 항종양 효과를 갖는 주요 대상으로 대두되고 있다. 이 연구에서는 혈관내피증식인자 수용체 억제제가 면역관문억제제의 항종양 효과를 향상시키는가 여부를 보여주기 위해 자궁경부암 마우스 모델에서 항마우스 세포사 단백질-1(항 PD-1)과 렌바티닙의 병용요법에 대한 효과를 확인하고자 한다.

연구재료와 연구방법

우리는 자궁경부암 마우스 모델을 설정하여 항 PD-1 과 렌바티닙 병용 요법에 따른 효과를 확인하였다. U14 세포 1×10^7 세포를 BALB/c 야생형 마우스와 BALB/c 누드 마우스의 측면에 피하 주사하였다. 면역 능력이 있는 마우스에서 종양 용적이 200 mm^3 에 도달하면 렌바티닙(10 mg/kg, 구강, 매일)을 복용하고 항 PD-1(마우스당 $200 \mu\text{g}$, 복강 내, 2 주간)으로 주입하였다. 종양의 부피는 일주일에 두 번 측정하였고 실험이 끝난 후 종양과 비장을 채취하여 조직학적 분석을 실시했다.

연구결과

면역능 모델(렌바티닙 278 mm^3 , 기준 490 mm^3)($p=0.0156$)에서 렌바티닙에 의해 종양의 크기가 유의하게 감소하였으며, 특히 2 주 이후 종양의 크기가 크게 감소하였다. 다음으로 면역능 모델에서 렌바티닙과 항 PD-1 의 병용 투여 효과를 조사하였다. 각각의 치료 그룹은 기준 그룹과 비교하여 다음과 같은 치료 효과를 나타냈다. (렌바티닙 278 mm^3 , 항 PD-1: 258 mm^3 , 기준그룹 490 mm^3) 또한 렌바티닙과 항 PD-1 을 병용투여한 군에서 종양 크기를 110 mm^3 감소시켰으며 각 단일 치료 그룹에 비교하여 유의한 차이를 보였다. ($p=0.0078$ and $p=0.0078$)

결론

이번 연구에서 항 PD-1의 항종양 효과는 면역 능력이 있는 자궁경부암 모델에서 렌바티닙과 병용 효과를 통한 종양 미세 환경의 변화를 통해 그 능력이 향상되었음을 확인할 수 있었다. 결론적으로 렌바티닙을 추가하면 내성이나 재발성 자궁경부암 환자에서 면역관문억제제의 효과가 향상될 것을 기대할 수 있다.